Organ-specific roles for transcription factor NF-κB in reovirus-induced apoptosis and disease

Sean M. O'Donnell,[1,2] Mark W. Hansberger,[2,3] Jodi L. Connolly,[2,3] James D. Chappell,[2,4] Melissa J. Watson,[1,2] Janene M. Pierce,[5] J. Denise Wetzel,[1,2] Wei Han,[6] Erik S. Barton,[2,3] J. Craig Forrest,[2,3] Tibor Valyi-Nagy,[2,4] Fiona E. Yull,[6] Timothy S. Blackwell,[6] Jeffrey N. Rottman,[6] Barbara Sherry,[7] and Terence S. Dermody[1,2,3]

[1]Department of Pediatrics, [2]Elizabeth B. Lamb Center for Pediatric Research, [3]Department of Microbiology and Immunology, [4]Department of Pathology, [5]Department of Surgery, and [6]Department of Medicine, Vanderbilt University School of Medicine, Nashville, Tennessee, USA. [7]Department of Molecular Biomedical Sciences, North Carolina State University, Raleigh, North Carolina, USA.

Reovirus induces apoptosis in cultured cells and in vivo. In cell culture models, apoptosis is contingent upon a mechanism involving reovirus-induced activation of transcription factor NF-κB complexes containing p50 and p65/RelA subunits. To explore the in vivo role of NF-κB in this process, we tested the capacity of reovirus to induce apoptosis in mice lacking a functional *nfkb1/p50* gene. The genetic defect had no apparent effect on reovirus replication in the intestine or dissemination to secondary sites of infection. In comparison to what was observed in wild-type controls, apoptosis was significantly diminished in the CNS of p50-null mice following reovirus infection. In sharp contrast, the loss of p50 was associated with massive reovirus-induced apoptosis and uncontrolled reovirus replication in the heart. Levels of IFN-β mRNA were markedly increased in the hearts of wild-type animals but not p50-null animals infected with reovirus. Treatment of p50-null mice with IFN-β substantially diminished reovirus replication and apoptosis, which suggests that IFN-β induction by NF-κB protects against reovirus-induced myocarditis. These findings reveal an organ-specific role for NF-κB in the regulation of reovirus-induced apoptosis, which modulates encephalitis and myocarditis associated with reovirus infection.

Introduction

Mechanisms of viral disease involve complex interactions of pathogen virulence factors and host responses. Perhaps the best-understood basis of organ-specific viral pathology is the availability of cell-surface molecules required for viral attachment and entry. Rarely, however, is viral disease ascribable solely to receptor recognition. More commonly, additional virus-host interactions determine the outcome of infection (1), and these pivotal steps are of much interest in studies of viral pathogenesis. Factors expected to modulate viral growth and virulence in an organ-dependent manner include the capacity of virus to efficiently utilize the host translational apparatus, including strategies to circumvent antiviral effects of IFN; availability of cellular proteins to facilitate viral replication and gene expression; and changes in the intracellular signaling dynamic induced by viral infection.

Mammalian orthoreoviruses (simply called reoviruses here) have served as highly tractable models for studies of viral pathogenesis. Reoviruses are nonenveloped, icosahedral viruses with a genome consisting of 10 double-stranded RNA segments (2). After infection of newborn mice, reoviruses disseminate systemically, producing injury to a variety of organs, including the CNS, heart, and liver (3). Strain-specific differences in receptor utilization influence some types of reovirus disease (4, 5); however, disease pathogenesis at other sites is more complex (6, 7).

Nonstandard abbreviations used: EMSA, electrophoretic mobility shift assay; HLL, HIV long-terminal repeat luciferase; L cell, L929 cell.

Conflict of interest: The authors have declared that no conflict of interest exists.

Citation for this article: *J. Clin. Invest.* **115**:2341–2350 (2005). doi:10.1172/JCI22428.

The NF-κB family of transcription factors plays a key role in the regulation of cell growth, activation, differentiation, and survival. Following exposure of cells to a variety of stimuli, NF-κB is activated and translocated to the nucleus (8), where it serves as a transcriptional regulator (9, 10). In systems in which NF-κB is activated during apoptosis, NF-κB can either prevent (10–13) or potentiate (14–17) cell death signaling. Following reovirus infection of cultured cells, the heterodimeric NF-κB complex p50/p65 translocates to the nucleus and activates proapoptotic gene expression (18). When NF-κB activation is inhibited using proteasome inhibitors or dominant-negative forms of IκBα, reovirus-induced apoptosis is blocked (18). Moreover, cell lines deficient in either of the p50 or p65 NF-κB subunits do not undergo apoptotic cell death following reovirus infection. These findings indicate that activation of NF-κB in cell culture is required for reovirus-induced apoptosis.

In the CNS (19) and heart (20) of newborn mice, reovirus induces the morphological and biochemical features of apoptosis. This cell-death response in brain and heart tissue is associated with reovirus-induced disease. Inhibitors of apoptosis ameliorate heart disease (20), which indicates a causal relationship between programmed cell death and reovirus-induced myocarditis. However, the molecular basis of CNS and cardiac pathology during reovirus infection has not been fully elucidated.

We now demonstrate that the p50 subunit of NF-κB plays an essential role in the development of encephalitis and myocarditis in reovirus-infected mice. Although reovirus infects the intestine and disseminates systemically following peroral inoculation of mice lacking the NF-κB p50 subunit, apoptosis is diminished in the brain yet strikingly enhanced in the heart. These findings sug-

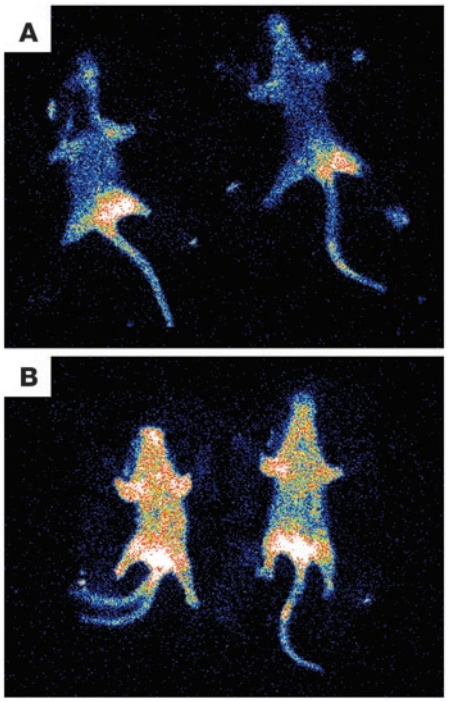

Figure 1
NF-κB activation following reovirus infection of HLL mice. Newborn HLL mice were inoculated perorally with PBS (**A**) or 10^4 PFU reovirus T3SA$^+$ (**B**). Mice were inoculated intraperitoneally with luciferin 7 days after infection and imaged for luciferase activity as a marker for NF-κB activation. Bioluminescence indicates areas of NF-κB activation.

gest a novel role for NF-κB in the pathogenesis of viral infection; it serves a proapoptotic function in the CNS, while mediating a prosurvival function in the myocardium.

Results

Reovirus activates NF-κB in vivo. To determine whether reovirus is capable of NF-κB activation in the intact host, we performed in vivo luciferase assays using transgenic mice engineered to express luciferase under control of an HIV long-terminal repeat promoter that contains NF-κB consensus binding sites (21). These mice were inoculated perorally with either PBS (mock-infected) or 10^4 PFU reovirus strain T3SA$^+$, which was chosen for these studies because of its capacity to activate NF-κB and induce a potent apoptotic response in cultured cells (22). Seven days after inoculation, the mice were imaged for luciferase activity as a marker for NF-κB activation (Figure 1, A and B). Little luciferase activity was detected in the mock-infected mice (Figure 1A). In contrast, reovirus-infected animals exhibited systemic luciferase activity (Figure 1B), which indicated that reovirus is capable of NF-κB activation in vivo.

Reovirus-induced activation of NF-κB in the murine CNS and heart is dependent on p50. To determine whether reovirus activates NF-κB in the murine CNS and heart, we performed electrophoretic mobility shift assays (EMSAs) using brain and heart extracts prepared from reovirus-infected or mock-infected wild-type and p50-null mice. Newborn p50$^{+/+}$ and p50$^{-/-}$ mice were inoculated with either PBS or 10^4 PFU reovirus T3SA$^+$. Cell extracts were prepared from brain and heart tissue 12 days after inoculation, incubated with a radiolabeled oligonucleotide consisting of the NF-κB consensus binding sequence, and resolved by PAGE using nondenaturing conditions (Figure 2, A and D). NF-κB DNA-binding activity was detected in extracts from the brain of reovirus-infected p50$^{+/+}$ but not p50$^{-/-}$ mice (Figure 2A). Similarly, NF-κB DNA-binding activity was detected in the heart of p50$^{+/+}$ mice infected with reovirus but not p50$^{-/-}$ animals (Figure 2D). These findings indicate that reovirus infection in the murine CNS and heart induces nuclear translocation of NF-κB, which is contingent on the expression of the NF-κB p50 subunit.

To confirm the specificity of NF-κB DNA-binding activity in these experiments, we incubated cell extracts from reovirus-infected p50$^{+/+}$ mouse brain and heart with a ^{32}P-labeled NF-κB consensus oligonucleotide in the presence of excess unlabeled consensus oligonucleotide (Figure 2, B and E). Binding of the radiolabeled probe was competed with that of unlabeled consensus oligonucleotide, which suggests that the gel-shift activity detected following reovirus infection is specific for sequences that are bound by NF-κB.

In cell culture, reovirus infection results in the nuclear translocation of NF-κB complexes containing subunits p50 and p65 (18). As an additional specificity control in these experiments for the activation of NF-κB, nuclear extracts were prepared from reovirus-infected p50$^{+/+}$ mouse brain or heart and incubated with an antiserum specific to p65 prior to the addition of the NF-κB–specific oligonucleotide (Figure 2, C and F). Addition of the p65-specific antiserum resulted in bands of higher relative molecular mass, which verified that p65 is present in the NF-κB complexes activated following reovirus infection. These findings provide strong evidence that reovirus infection of the murine CNS induces the nuclear translocation of NF-κB and this effect is abolished in mice lacking p50.

NF-κB subunit p50 is not required for efficient reovirus replication or dissemination in the murine host. To determine whether p50 plays a role in reovirus growth in vivo, we inoculated p50$^{+/+}$ and p50$^{-/-}$ mice intracranially or perorally with 10^4 PFU reovirus T3SA$^+$. Viral titers in the brain were determined by plaque assay 2, 4, and 6 days after intracranial inoculation (Figure 3A) and in the intestine, liver, brain, and heart 4, 6, 8, 10, and 12 days after peroral inoculation (Figure 3B). Following intracranial inoculation, viral titers in p50$^{+/+}$ and p50$^{-/-}$ mice were equivalent at all time points tested. After peroral inoculation, virus replicated efficiently in the intestines of both p50$^{+/+}$ and p50$^{-/-}$ mice and disseminated to the liver, brain, and heart. Viral titers in the intestine, liver, and brain did not differ between p50$^{+/+}$ and p50$^{-/-}$ mice. In sharp contrast, viral titers in the hearts of p50$^{-/-}$ mice were more than 1,000-fold higher than those in the hearts of p50$^{+/+}$ animals. These findings suggest that p50 is dispensable for reovirus growth in vivo and that the absence of p50 in the heart, but not in other tissues tested, allows for increased reovirus replication.

NF-κB subunit p50 is required for efficient induction of apoptosis in the CNS following reovirus infection. To assess reovirus-induced pathologic changes in the CNS of p50$^{+/+}$ and p50$^{-/-}$ mice, we prepared brain sections from mice euthanized at 12 days following peroral inoculation with reovirus T3SA$^+$ and examined them after staining with H&E (Figure 4, A and B and data not shown). Brain sections from reovirus-infected p50$^{+/+}$ and p50$^{-/-}$ mice exhibited evidence of meningoencephalitis. Inflammatory infiltrates were detected primarily in the cerebral cortex, hippocampus, diencephalon, and brain stem. Morphologically, inflammatory cells were mostly lymphocytes and macrophages/microglia with some plasma cells and neutrophils. Inflammatory changes were more extensive in p50$^{+/+}$ mice (Figure 4A) than in p50$^{-/-}$ mice (Figure 4B),

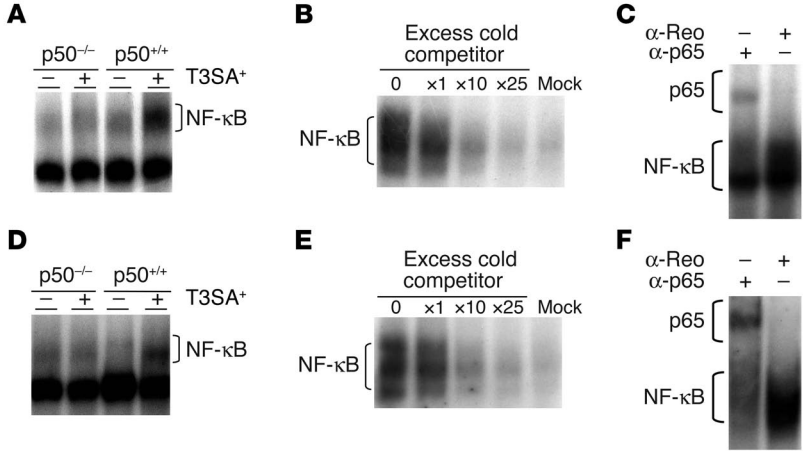

Figure 2

Reovirus-induced NF-κB gel-shift activity following infection of $p50^{+/+}$ and $p50^{-/-}$ mice. (**A** and **D**) Newborn $p50^{+/+}$ and $p50^{-/-}$ mice were inoculated perorally with either 10^4 PFU reovirus $T3SA^+$ or PBS. Brains (**A**) and hearts (**D**) were resected 12 days after inoculation, and cell extracts were prepared. Extracts were incubated with a ^{32}P-labeled NF-κB consensus oligonucleotide and resolved by nondenaturing PAGE. Activated NF-κB complexes are indicated. Shown is a representative experiment of 4 performed. (**B** and **E**) Extracts were prepared from either brains (**B**) or hearts (**E**) of reovirus-infected $p50^{+/+}$ mice and incubated with ^{32}P-labeled NF-κB consensus oligonucleotide in the presence of unlabeled NF-κB consensus probe (cold competitor) at the molar concentrations shown. Extracts prepared from either brains or hearts of uninfected $p50^{+/+}$ mice were incubated with ^{32}P-labeled NF-κB consensus oligonucleotide and electrophoresed in the lane labeled "Mock." NF-κB complexes are indicated. (**C** and **F**) Extracts were prepared from either brains (**C**) or hearts (**F**) of reovirus-infected $p50^{+/+}$ mice, and prior to the addition of the ^{32}P-labeled oligonucleotide probe, extracts were incubated with either a control antibody specific to reovirus protein σ3 (α-Reo) or an antibody specific to NF-κB subunit p65 (α-p65). Supershifted complexes containing p65 are indicated.

which suggests that the neurovirulence of reovirus is attenuated in mice lacking an intact NF-κB signaling apparatus.

To assess the distribution of reovirus protein expression in the CNS of $p50^{+/+}$ and $p50^{-/-}$ mice, we prepared brain sections from mice euthanized 12 days following peroral inoculation and stained them using a reovirus-specific antiserum (Figure 4, A and B and data not shown). Immunohistochemical staining for reovirus protein demonstrated the presence of immunoreactive neurons in brains of both $p50^{+/+}$ and $p50^{-/-}$ mice (Figure 4, A and B). Antigen-positive neurons were detected in a pattern recapitulating the inflammatory changes; the cerebral cortex, hippocampus, diencephalon, and brain stem were primarily involved. The number of reovirus-infected cells and their distribution was similar in $p50^{+/+}$ and $p50^{-/-}$ mice (Figure 4, A and B). These results suggest that the lack of p50 does not alter reovirus tropism for specific neural regions.

To determine whether p50 is required for apoptosis in the murine CNS, we prepared brain sections from reovirus-infected $p50^{+/+}$ and $p50^{-/-}$ mice 12 days following peroral inoculation (Figure 4, A and B) or 6 days following intracranial inoculation (Figure 4C) and assayed them for fragmented DNA using the TUNEL technique. Apoptotic cells were quantitated by counting all TUNEL-positive cells in cortex, hippocampus, basal ganglia, diencephalon, and brain stem of each section obtained from mice inoculated intracranially (Figure 5). Numbers of TUNEL-positive cells in the brains of infected $p50^{+/+}$ mice were significantly greater than those in the brains of infected $p50^{-/-}$ mice. These findings were the same following both peroral and intracranial inoculation (Figure 4). Thus, reovirus-induced apoptosis in the murine CNS is dependent on the p50 subunit of NF-κB.

Activation of caspase-3 is a highly specific biomarker of apoptotic cell death (23). To confirm that DNA fragmentation observed in the brains of reovirus-infected $p50^{+/+}$ mice is due to apoptosis, we stained brain sections with an antiserum specific to the activated form of caspase-3 (Figure 4, A and B). Activated caspase-3 was detected in regions of the brain in which TUNEL-positive staining also was observed. Moreover, cells immunoreactive for caspase-3 were detected at a much higher frequency in the brains of $p50^{+/+}$ mice. Morphologically, cells immunoreactive for caspase-3 were primarily neurons, and most immunoreactive neurons also exhibited morphologic evidence of apoptosis. These results provide additional evidence that expression of NF-κB subunit p50 is required for efficient induction of apoptosis during reovirus infection in the murine CNS.

Absence of NF-κB subunit p50 leads to enhanced pathology and massive apoptosis in the murine heart following reovirus infection. Since viral titers in the hearts of $p50^{-/-}$ mice were more than 1,000-fold higher than in those of $p50^{+/+}$ mice (Figure 3B), we examined heart tissue for evidence of inflammation and tissue injury. Newborn $p50^{+/+}$ and $p50^{-/-}$ mice were inoculated perorally with either 10^4 PFU reovirus $T3SA^+$ or PBS and weighed daily. Mice were euthanized at various time points following inoculation, and hearts were removed and weighed. There were no significant differences in the heart weights of mock-infected $p50^{+/+}$ and $p50^{-/-}$ mice (Figure 6A). Surprisingly, heart weights of reovirus-infected $p50^{-/-}$ mice were significantly greater than those of $p50^{+/+}$ mice (Figure 6B). Differences in the percent heart weight (heart weight relative to total body weight) of infected $p50^{+/+}$ and $p50^{-/-}$ mice became detectable at 8 days after inoculation and continued to increase with time, while there was no significant increase in the percent heart weight of infected $p50^{+/+}$ mice (Figure 6B). Dramatic differences were observed in the gross appearance of hearts dissected from $p50^{+/+}$ and $p50^{-/-}$ animals following infection with reovirus (Figure 6C). Hearts from reovirus-infected $p50^{-/-}$ mice had a blanched appearance with diffuse surface irregularities corresponding to confluence of purulent lesions, consistent with overt myocarditis. In contrast, hearts from mock-infected $p50^{-/-}$ or $p50^{+/+}$ mice or reovirus-infected $p50^{+/+}$ mice displayed no overt abnormalities.

To determine whether reovirus-induced myocardial injury in $p50^{-/-}$ mice is associated with contractile dysfunction, we performed echocardiography on 10-day-old mice after peroral inoculation with either reovirus $T3SA^+$ or PBS. Fractional shortening, assessed by 2-dimensional, directed M-mode measurements, was substantially decreased in reovirus-infected $p50^{-/-}$ mice (~10%; Figure 6D), while it was preserved in mock-infected $p50^{-/-}$ mice (>40%; Figure 6E) and reovirus-infected $p50^{+/+}$ mice (>40%; Figure 6F). Heart size was also increased in reovirus-infected $p50^{-/-}$ mice compared with mock-infected $p50^{-/-}$ mice and reovirus-infected $p50^{+/+}$ mice. Intact atrioventricular conduction was observed in all mice, which suggests that the pathologic process was not specifically

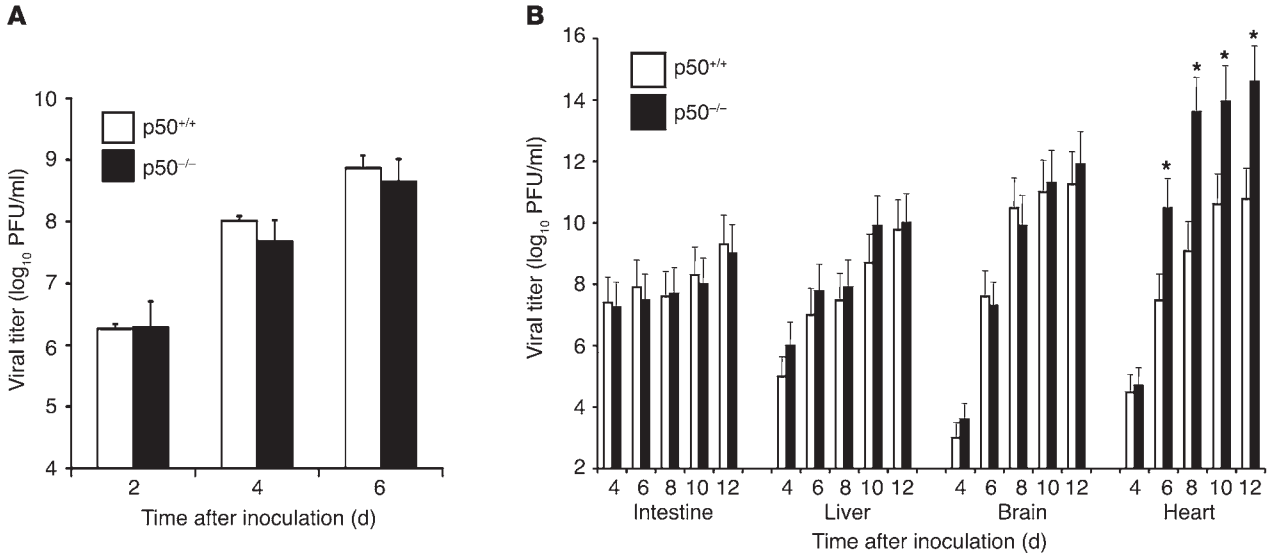

Figure 3
Growth of reovirus in p50$^{+/+}$ and p50$^{-/-}$ mice. (**A**) Titers of reovirus in brain after intracranial inoculation of p50$^{+/+}$ and p50$^{-/-}$ mice. Newborn mice were inoculated with 10^4 PFU reovirus T3SA$^+$. At days 2, 4, and 6 after inoculation, mice were euthanized, brains were harvested, and viral titers were determined by plaque assay. (**B**) Titers of reovirus in intestine, liver, brain, and heart after peroral inoculation of p50$^{+/+}$ and p50$^{-/-}$ mice. Newborn mice were inoculated with 10^4 PFU T3SA$^+$. At days 4, 6, 8, 10, and 12 after inoculation, mice were euthanized, organs were harvested, and viral titers were determined by plaque assay. The results are expressed as the mean viral titers for 2–4 (**A**) or 4–8 (**B**) animals for each time point. Error bars indicate SDs. *$P < 0.05$ by Student's *t* test.

targeted to the conduction system. These results suggest that the myocardial pathology associated with reovirus infection of p50$^{-/-}$ mice is associated with diminished contractility.

On a microscopic level, hearts of p50$^{-/-}$ animals displayed extensive myocyte destruction with features of apoptotic and necrotic cell death. Affected areas were notable for cell fragments, granular debris, and scattered calcifications. Thorough sectioning of the organ block revealed that pathology was not limited to any particular region of the heart. Hearts from reovirus-infected p50$^{+/+}$ mice and mock-infected p50$^{-/-}$ and p50$^{+/+}$ mice demonstrated no significant microscopic pathology. We conclude that reovirus is more pathogenic in the heart in the absence of NF-κB subunit p50.

To assess the extent and location of reovirus infection in the murine myocardium in the presence and absence of p50, we performed reovirus antigen staining on heart sections from p50$^{+/+}$ and p50$^{-/-}$ mice euthanized 12 days following peroral inoculation with reovirus T3SA$^+$ (Figure 7, A and B). Immunohistochemical staining for reovirus protein demonstrated immunoreactive myocytes in heart sections prepared from both p50$^{+/+}$ and p50$^{-/-}$ mice (Figure 7, A and B). However, the number of reovirus-infected cells differed substantially between p50$^{+/+}$ and p50$^{-/-}$ mice, consistent with the significant difference in viral titer in the hearts of these animals.

To determine whether expression of p50 influences apoptosis in the murine heart, we inoculated p50$^{+/+}$ and p50$^{-/-}$ mice perorally with reovirus and assessed them for apoptosis using TUNEL staining (Figure 7, A and B). There were rare TUNEL-positive cells in the hearts of p50$^{+/+}$ mice following reovirus infection (Figure 7A), whereas numerous foci of apoptosis were present in the hearts of p50$^{-/-}$ mice (Figure 7B). Interestingly, foci of apoptotic cells in the hearts of p50$^{-/-}$ mice coincided with areas of intense staining for reovirus antigen, which suggests a link between reovirus replication and apoptosis in cardiomyocytes.

To confirm that the absence of p50 leads to enhanced apoptosis in the heart during reovirus infection, we prepared heart sections from p50$^{+/+}$ and p50$^{-/-}$ mice 12 days following peroral inoculation with reovirus and stained them for activated caspase-3 (Figure 7, A and B). Caspase-3 staining revealed numerous positive myocytes in the same areas of the heart that also were positive for reovirus antigen and TUNEL staining. These results suggest that, in contrast to its effects in the murine CNS, the NF-κB p50 subunit protects against apoptosis induced by reovirus infection in the murine myocardium.

IFN-β is induced in the heart of wild-type mice following reovirus infection. Results presented thus far demonstrate that enhanced reovirus growth in the heart of p50$^{-/-}$ mice is associated with massive apoptosis. We thought it possible that the absence of NF-κB–mediated activation of innate immune responses might lead to increased viral replication and resultant pathology in the heart. To test this hypothesis, we inoculated p50$^{+/+}$ and p50$^{-/-}$ mice perorally with reovirus T3SA$^+$ or PBS. Twelve days after inoculation, heart and brain were removed, and levels of IFN-β mRNA were determined using real-time PCR (Figure 8). Using GAPDH mRNA as a standardization control, little IFN-β mRNA was induced in the brain of either p50$^{-/-}$ or p50$^{+/+}$ mice in the presence or absence of reovirus infection (Figure 8). In contrast, IFN-β mRNA levels were substantially increased in the heart of reovirus-infected wild-type mice compared with p50$^{-/-}$ animals (Figure 8). These results indicate that IFN-β induction by reovirus in the murine heart is dependent on NF-κB and suggest that IFN-β protects the heart from reovirus-induced apoptosis and disease.

IFN-β treatment of p50-null mice attenuates reovirus-induced myocarditis. To determine whether NF-κB–mediated expression of IFN-β plays a direct role in protection of the heart against apoptosis and disease caused by reovirus, we tested the effect of IFN-β treatment on reovirus infection of p50$^{-/-}$ mice. Newborn p50$^{-/-}$ mice were inoculated intraperitoneally with either IFN-β or PBS 1 day prior

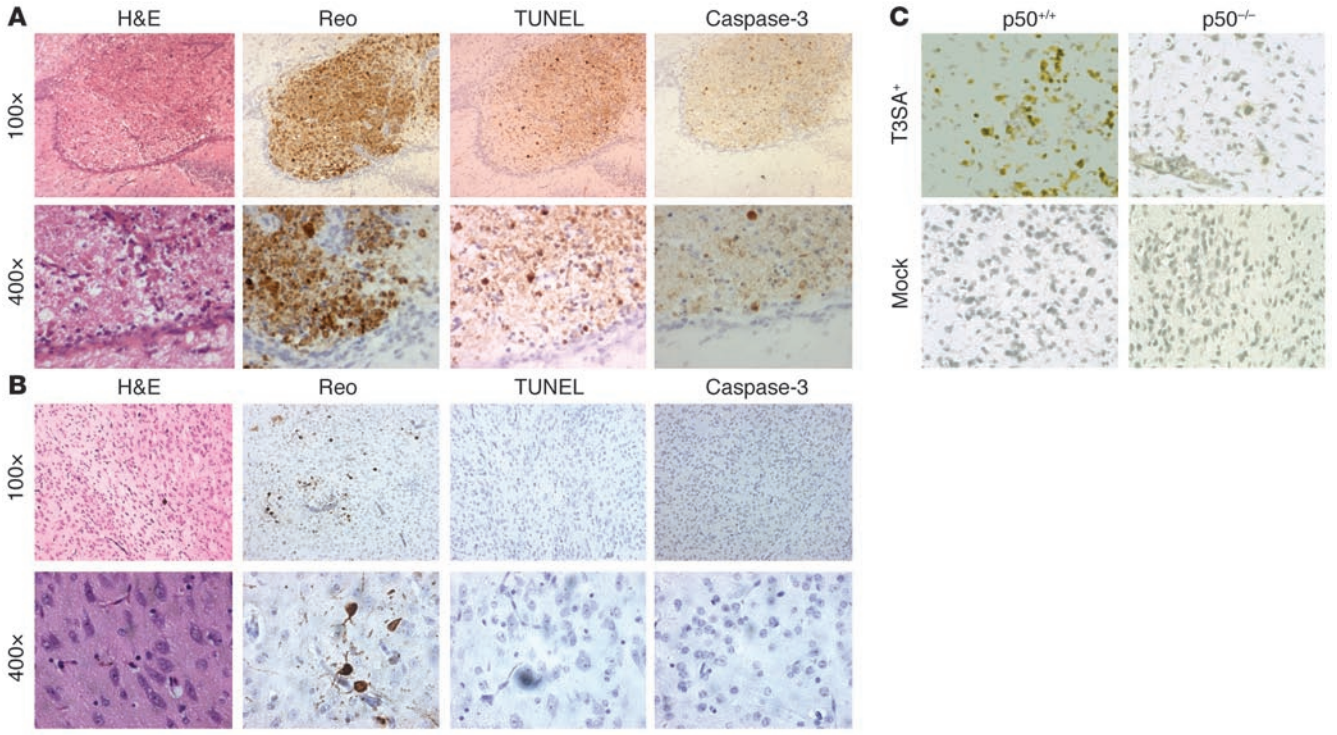

Figure 4
Inflammation, reovirus protein expression, TUNEL staining, and immunohistochemical detection of activated caspase-3 in the brain of reovirus-infected $p50^{+/+}$ (**A**) and $p50^{-/-}$ (**B**) mice. Newborn mice were inoculated perorally with 10^4 PFU reovirus T3SA+. At 12 days after inoculation, brains were harvested, paraffin embedded, sectioned, and stained with H&E, polyclonal reovirus-specific antiserum (Reo), TUNEL, or activated caspase-3–specific antiserum as indicated. Shown are consecutive sections of diencephalon. Original magnification, ×100 (top panels) and ×400 (bottom panels). (**C**) Newborn mice were inoculated intracranially with 10^4 PFU T3SA+ or gelatin saline (Mock). At 6 days after inoculation, mice were euthanized, and brain sections were stained using a TUNEL assay. Shown are sections of the upper brain stem. Original magnification, ×200. Brown staining indicates reovirus protein, fragmented DNA, or activated caspase-3.

to peroral inoculation with reovirus T3SA+ and treated daily for 9 days thereafter. On day 10, the animals were euthanized, and brain and heart were removed for determination of viral titer and histopathology (Figure 9). IFN-β treatment significantly decreased viral titer in both brain and heart (Figure 9A). In $p50^{-/-}$ mice treated with IFN-β, viral titers reached only 10^2 PFU in the brain and were less than 10^2 PFU in the heart (Figure 9A). In parallel with these results, apoptosis in the heart of IFN-β–treated $p50^{-/-}$ mice was substantially diminished (Figure 9B). Thus, a critical component of the underlying mechanism of NF-κB–mediated protection against reovirus-induced myocardial injury is contingent on IFN-β.

Discussion

Here we report organ-specific roles for NF-κB in the pathogenesis of viral disease, which is a heretofore unknown property of this signaling molecule. The key finding is that marked differences in the pathogenesis of reovirus infection in the CNS and heart are dependent on the action of NF-κB. Following reovirus infection in the CNS, $p50^{+/+}$ mice exhibited significant neuronal apoptosis, while $p50^{-/-}$ mice displayed a minimal apoptotic response. In sharp contrast, reovirus induced little apoptosis in the heart of $p50^{+/+}$ mice, whereas extensive apoptosis occurred in the heart of $p50^{-/-}$ mice. These findings indicate that NF-κB subunit p50 plays 2 distinctly different roles in reovirus pathogenesis, serving a proapoptotic function in the brain, while mediating a prosurvival function in the heart.

The NF-κB family of transcription factors is composed of p50/p105, p52/p100, p65 (RelA), c-Rel, and RelB. Studies using mice with targeted disruptions of specific NF-κB subunits have shown that NF-κB serves important functions in the development and function of innate and adaptive immunity (24–26). Mice lacking p50 have no apparent developmental defects (24), and immune cells mature normally. However, $p50^{-/-}$ mice display defects in B cell activation, isotype switching, and antibody production (24). These defects render $p50^{-/-}$ mice more susceptible to infection by the Gram-positive bacterial pathogen *Streptococcus pneumoniae*, but they remain capable of efficiently clearing infection by the Gram-negative pathogens *Escherichia coli* and *Haemophilus influenzae* (24). When $p50^{-/-}$ mice are infected with encephalomyocarditis virus, they are actually more resistant to infection than controls. This difference is thought to be due to an increase in apoptosis that leads to a decrease in viral growth (24). These findings stand in stark contrast to what occurs in the CNS and heart of reovirus-infected mice.

In experiments comparing reovirus infection of $p50^{+/+}$ and $p50^{-/-}$ mice, we found that the presence or absence of p50 did not alter primary viral replication in intestinal tissue or dissemination of virus to the liver, brain, or heart. Although viral replication in the brain after intracranial inoculation also was independent of p50, replication in the heart was increased in $p50^{-/-}$ mice by approximately 1,000-fold. What might explain the enhancement of reovirus replication in the heart of $p50^{-/-}$ mice? Reovirus strains have

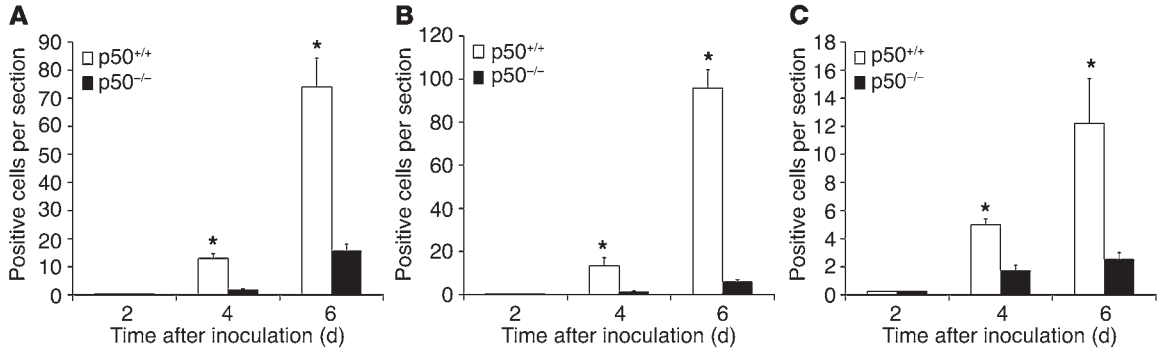

Figure 5
Quantitation of TUNEL staining in cortex and hippocampus (**A**), basal ganglia and diencephalon (**B**), and brain stem (**C**) of reovirus-infected $p50^{+/+}$ and $p50^{-/-}$ mice. TUNEL staining was performed using tissue sections prepared 2, 4, and 6 days following intracranial inoculation of $p50^{+/+}$ and $p50^{-/-}$ mice with 10^4 PFU reovirus T3SA+. For each brain region, all positive cells in a single parasagittal section were counted for 4–8 animals. The results are expressed as the mean number of apoptotic cells per region. Error bars indicate SDs. *$P < 0.05$ by Student's t test.

been characterized previously as having the capacity to grow in the murine heart and produce cardiac disease (27, 28). In primary cardiomyocytes, nonmyocarditic reovirus strains induce more IFN-β and are more sensitive to the antiviral effects of this cytokine than myocarditic reovirus strains (29). Furthermore, normally nonmyocarditic strains are capable of producing myocarditis in infected IFN-α/β$^{-/-}$ mice (29). Thus, it appears that type I IFNs restrict viral replication in the heart and attenuate cardiac disease.

NF-κB is known to induce the expression of several mediators of innate immune responses including type I IFNs (30–32). Therefore, absence of p50 may allow reovirus to achieve much higher titers and cause myocarditis. We tested this hypothesis by determining brain and heart levels of IFN-β mRNA in response to reovirus infection of $p50^{+/+}$ and $p50^{-/-}$ mice (Figure 8) and by treating reovirus-infected $p50^{-/-}$ mice with IFN-β (Figure 9). In these experiments, we found a dramatic increase in IFN-β expression in the hearts of wild-type mice but only a minimal IFN-β response in the hearts of p50-null animals. Moreover, reconstitution of $p50^{-/-}$ mice with IFN-β substantially diminished reovirus replication and apoptosis, which resulted in diminished myocardial injury. These results indicate that IFN-β is a necessary component of the NF-κB–mediated protective response against reovirus in the heart. However, it is likely that other components of innate immunity are involved in this effect. Preliminary data from our laboratory suggest that in addition to IFN-β, IL-6, MIF, and TNF are expressed at higher levels in the heart of $p50^{+/+}$ mice than $p50^{-/-}$ mice (S.M. O'Donnell and T.S. Dermody, unpublished observation). These findings suggest that following reovirus infection of the heart, NF-κB is activated and leads to induction of potent innate immune responses, which in turn attenuate viral replication at that site, resulting in diminished apoptosis and disease.

The enhanced growth of reovirus in the heart of $p50^{-/-}$ mice compared with $p50^{+/+}$ mice was associated with extensive myocarditis and resultant tissue injury and dysfunction. This result was confirmed by histopathological studies, echocardiography, and physical examination revealing signs of heart failure. The pathology observed in the heart of $p50^{-/-}$ animals was characterized by extensive tissue damage and little inflammatory infiltrate, similar to findings made in previous studies of reovirus myocarditis (27). Therefore, our results suggest that apoptosis is the primary mechanism of cardiac damage in reovirus-induced myocarditis, as reported previously (20). Damage to cardiomyocytes during reovirus infection occurs in the complete absence of adaptive components of host defense (33). It is possible that a similar mechanism occurs in humans, which would explain why some patients with acute myocarditis develop heart failure in the setting of sustained viremia (34).

In contrast to the enhanced growth of reovirus in the heart of $p50^{-/-}$ mice, viral growth in the CNS of $p50^{+/+}$ and $p50^{-/-}$ mice was equivalent. However, we observed dramatic differences in the number of apoptotic cells in the 2 mouse strains as indicated by TUNEL and caspase-3 staining. Therefore, the efficiency of viral growth is not strictly correlated with the extent of the apoptotic response. Nonetheless, despite these p50-dependent differences in viral growth, our results suggest that apoptosis is an important mechanism of reovirus-induced disease in both the CNS and heart. In the CNS of $p50^{-/-}$ mice, apoptosis and inflammation following reovirus infection were diminished. However, in the hearts of these animals, apoptosis and tissue injury were enhanced. This correlation between apoptosis and pathology lends support to the hypothesis that therapies directed at blocking programmed cell death might attenuate viral virulence, consistent with results from previous studies of reovirus-induced myocarditis (20). However, our findings suggest that pharmacologic inhibition of NF-κB activation may reduce pathologic injury at some sites and exacerbate disease at others, depending on the nature of the NF-κB agonist.

The precise cell types responsible for the p50-dependent effects on apoptosis in response to reovirus infection in mice are not apparent from our study. It is possible that expression of p50 in neurons is required for apoptosis of these cells and expression of p50 in cardiomyocytes mediates protection of these cells against apoptotic injury. However, it is also possible that p50-dependent immune responses contribute to the observed differences in cell fate. For example, NF-κB–mediated release of cytokines such as TNF-α from immune cells might contribute to the neuronal apoptosis that occurs during reovirus infection of the CNS, whereas NF-κB–mediated release of type I IFNs from immune cells might mediate a protective effect in the heart. Since adoptive transfer of immune cells is not technically feasible in the newborn mice required for studies of reovirus pathogenesis, discrimination between these possibilities awaits the development of mice with tissue-specific ablation of NF-κB activity.

The role of NF-κB in response to a variety of cellular stresses has been studied extensively using cultured cells (35). However, little is known about the contributions of specific NF-κB subunits in vivo.

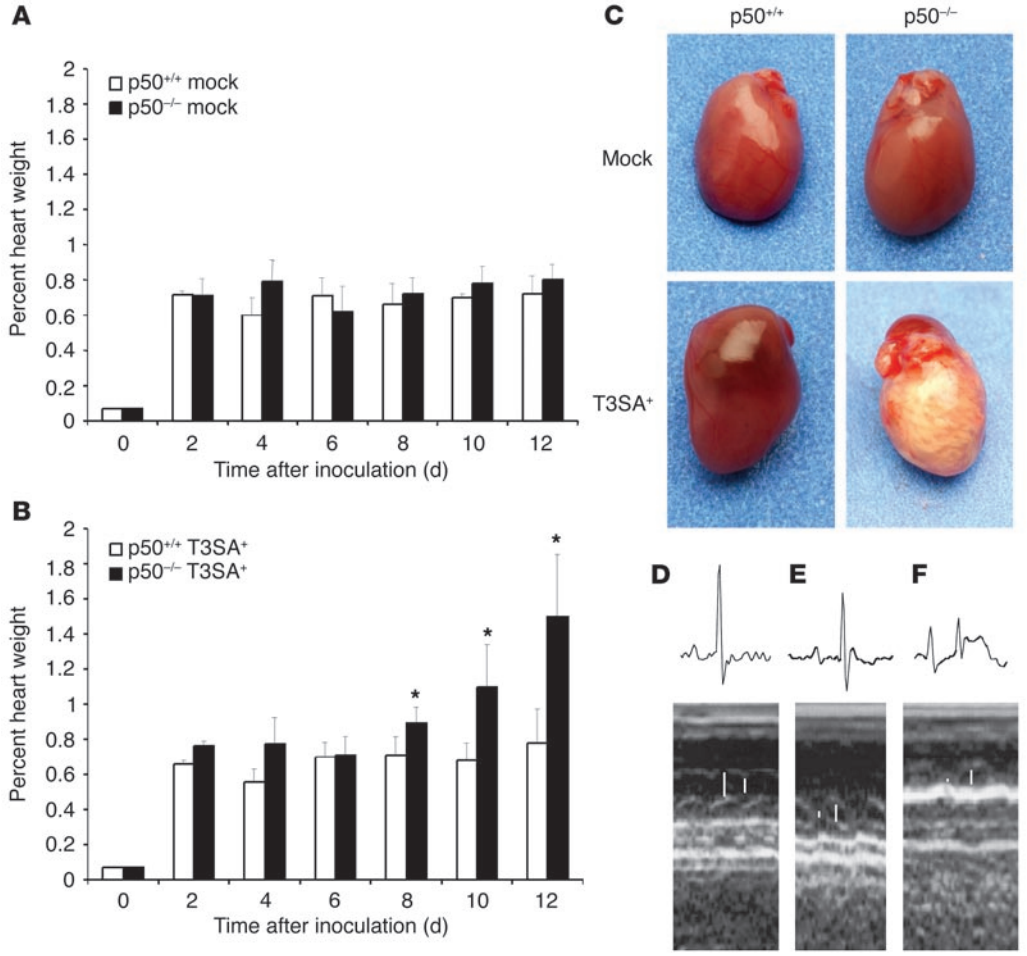

Figure 6
Heart pathology following reovirus infection of p50$^{+/+}$ and p50$^{-/-}$ mice. (**A** and **B**) Newborn p50$^{+/+}$ and p50$^{-/-}$ mice were inoculated perorally with either PBS (mock) (**A**) or 10^4 PFU reovirus T3SA$^+$ (**B**), and heart size was monitored at 2-day intervals. Percent heart weight was calculated as heart weight divided by body weight. The results are expressed as the mean heart weights of at least 4 animals for each time point. Error bars indicate SDs. *$P < 0.05$ by Student's *t* test. (**C**) Hearts from mice euthanized 12 days following peroral inoculation with reovirus T3SA$^+$ or gelatin saline (Mock). (**D**, **E**, and **F**) Electrocardiography and echocardiography of reovirus-infected p50$^{-/-}$ (**D**), mock-infected p50$^{-/-}$ (**E**), and reovirus-infected (**F**) p50$^{+/+}$ mice. Newborn mice were inoculated perorally with 10^4 PFU T3SA$^+$, and tests were performed 10 days after inoculation. A P-wave/QRS ECG complex is displayed above the corresponding echocardiographic image. Systolic and diastolic LV cavity dimensions are indicated by bars superimposed on the M-mode images.

The extensive array of NF-κB inducers and target genes (36) suggests that numerous mechanisms exist to direct transcription of appropriate NF-κB–dependent genes in response to specific stimuli. One such regulatory mechanism is likely to be the activation of specific NF-κB complexes (e.g., p50/p65 heterodimers) for each inducing signal. Individual homodimeric and heterodimeric NF-κB complexes exhibit different affinities for target DNA sequences (37), and this provides a potential mechanism by which NF-κB–inducing stimuli regulate transcriptional activity of specific subsets of cellular genes. We showed previously that reovirus requires p50/p65 for efficient apoptosis in cell culture (18). However, we found in the current study that p50 plays organ-specific roles in disease pathogenesis in vivo. These findings emphasize that NF-κB subunits can have different functions following activation with the same stimulus depending on the cellular environment. Continuing studies in this area may reveal new layers of control of NF-κB responses and extend understanding of how viruses cause tissue-specific injury.

Methods

Cells, virus, and antibodies. Spinner-adapted murine L929 cells (L cells) were grown in suspension or monolayer culture and maintained as described previously (18). Reovirus strain T3SA$^+$ was generated by reassortment of reovirus strains type 1 Lang (T1L) and type 3 clone 44-MA (5). Virus was purified after growth in L cells by cesium chloride gradient centrifugation (38). Rabbit polyclonal anti-reovirus serum raised against strain T1L was obtained as described previously (22). Rabbit polyclonal antiserum specific to the activated form of caspase-3 (anti–caspase-3/Asp 175) was obtained from Cell Signaling Technology.

Mice and inoculations. HIV long-terminal repeat luciferase (HLL) mice were generated as described previously (39). Control p50$^{+/+}$ mice (B6129PF1/J-A$^{W\text{-}J}$/A^W) and p50$^{-/-}$ mice (B6129P-Nfkb1^{tm1Bal}) (24) were obtained from The Jackson Laboratory. Newborn mice weighing 2.0–2.5 g (2–4 days old) were inoculated either intracranially or perorally with purified T3SA$^+$ diluted in PBS. Intracranial inoculations were delivered to the right and left cerebral hemispheres (5 μl each) using a Hamilton syringe (BD Biosciences) and a 30-gauge needle (40). Peroral inoculations were delivered into the stomach (50 μl) by passage of a polyethylene catheter 0.61 mm in diameter (BD) through the esophagus (41). The inoculum contained 0.5% (vol/vol) green food coloring so that accuracy of delivery could be judged. For determination of NF-κB activation, viral titer, and immunohistochemical staining, mice were euthanized at various intervals following inoculation, and organs were collected.

Assessment of NF-κB activation by in vivo luciferase activity. Two-day-old HLL mice were inoculated perorally with either 10^4 PFU T3SA$^+$ or PBS. Mice were anesthetized with isoflurane before imaging and immobilized for the duration of the integration time of photon counting (3 minutes). Luciferin (0.75 g/mouse in 0.2 ml isotonic saline) was inoculated intraperitoneally, and mice were imaged using an intensified charge-coupled devise camera (C2400-32; Hamamatsu Corp.). For the duration of photon counting, mice were placed inside a light-tight box. Light

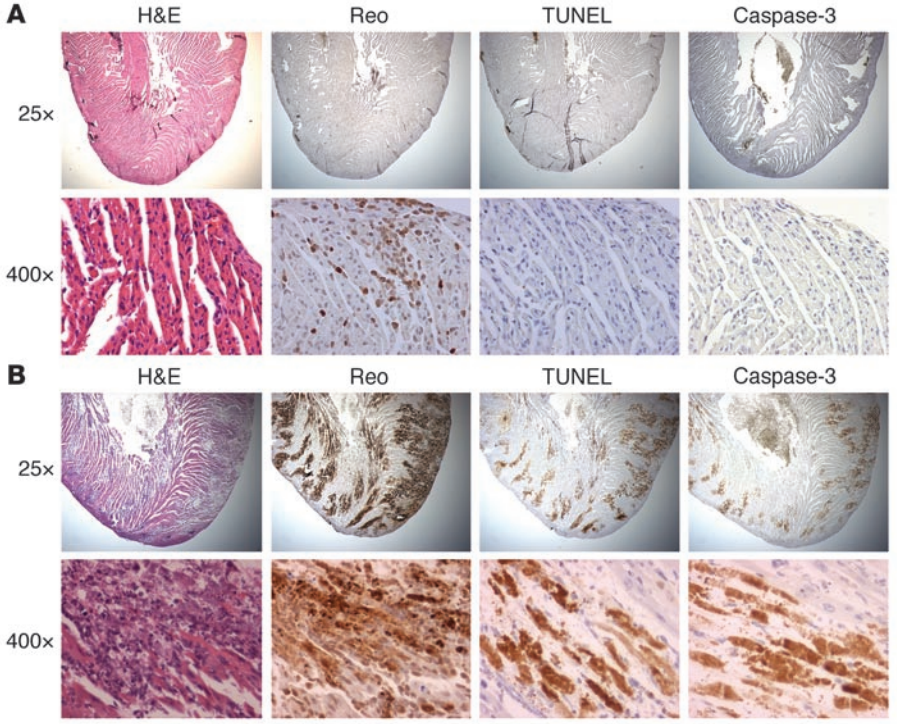

Figure 7
Inflammation, reovirus protein expression, TUNEL staining, and immunohistochemical detection of activated caspase-3 in the heart of reovirus-infected $p50^{+/+}$ (**A**) and $p50^{-/-}$ mice (**B**). Newborn mice were inoculated perorally with 10^4 PFU reovirus $T3SA^+$. At 12 days after inoculation, hearts were harvested, paraffin embedded, sectioned, and stained with H&E, polyclonal reovirus-specific antiserum, TUNEL, or activated caspase-3–specific antiserum as indicated. Original magnification, ×25 (top panels) and ×400 (bottom panels). Brown staining indicates reovirus protein, fragmented DNA, or activated caspase-3.

emission from each mouse was detected as photon counts, and a digital false-color photon emission image of the mouse was generated.

EMSAs. Two-day-old $p50^{+/+}$ and $p50^{-/-}$ mice were inoculated perorally with either 10^4 PFU $T3SA^+$ or PBS. Mice were euthanized 12 days after inoculation. Brains and hearts were aseptically removed, snap frozen on dry ice, and stored at –70°C. Organs were weighed, placed in a mortar with liquid nitrogen, and ground into a powder. Lysis buffer (20 mM HEPES [pH 7.9], 25% glycerol, 0.42 M NaCl, 1.5 mM $MgCl_2$, 0.2 mM EDTA, 0.5 mM phenylmethylsulfonyl fluoride, 0.5 mM dithiothreitol) was added in a ratio of 1 ml per 200 mg of tissue. Samples were frozen and thawed 3 times and centrifuged at 12,000 *g* for 10 minutes. The supernatant was used as the whole-cell extract.

Whole-cell extracts (10 μg total protein) were assayed for NF-κB activation by EMSA using a ^{32}P-labeled oligonucleotide (1.0 ng) consisting of the NF-κB consensus binding sequence (Santa Cruz Biotechnology Inc.) as described previously (18). For competition experiments, unlabeled consensus oligonucleotide at various concentrations was added to the reaction mixtures along with radiolabeled oligonucleotide. For supershift experiments, 1 μl of a rabbit polyclonal antiserum specific to p65 (250 μg/ml; Santa Cruz Biotechnology Inc.) was added to the binding reaction mixtures and incubated at 4°C for 30 minutes prior to the addition of radiolabeled oligonucleotide. Nucleoprotein complexes were subjected to electrophoresis in native polyacrylamide gels, which were dried and exposed to film.

Determination of viral titer in infected organs. Organs (intestine, liver, heart, and brain) from infected $p50^{+/+}$ and $p50^{-/-}$ mice were placed into vials containing 1 ml gelatin saline, frozen (–20°C) and thawed once, and sonicated for 20 seconds. Titers of virus present in organ homogenates were determined by plaque assay using L cell monolayers (42).

Histology, immunohistochemistry, and TUNEL staining. Litters of newborn $p50^{+/+}$ and $p50^{-/-}$ mice were inoculated intracranially or perorally with either 10^4 PFU $T3SA^+$ or PBS. Mice were euthanized, and brain and heart tissues were fixed in 10% buffered paraformaldehyde. Fixed organs were embedded in paraffin, and 6-μm histological sections were prepared. Sections were stained with H&E for evaluation of histopathologic changes, processed for immunohistochemical detection of reovirus protein, assayed for DNA fragmentation using the TUNEL technique (43), or processed for the immunohistochemical detection of activated caspase-3 (5). Cells demonstrating TUNEL staining were quantitated separately in each parasagittal brain section in the following regions: cerebral cortex, hippocampus, basal ganglia, diencephalon, and brain stem. The mean number of positive cells per region was determined for each treatment group and time point. Observers were blinded to the identity of the mouse strain and the nature of the inoculum.

Echocardiography. Echocardiography was performed on conscious 10-day-old pups as previously described for adult mice (44) except that the total field depth was set to 1 cm (minimum possible), and external heating and rapid

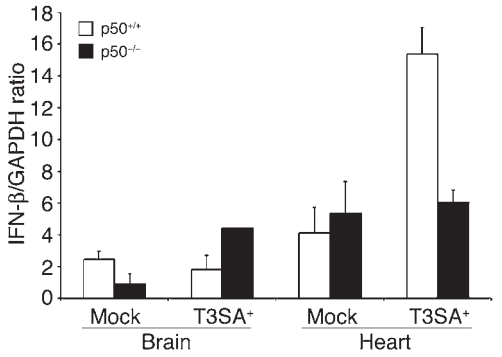

Figure 8
Levels of IFN-β mRNA in brain and heart of $p50^{+/+}$ and $p50^{-/-}$ mice. Newborn mice were inoculated perorally with either PBS (Mock) or 10^4 PFU reovirus $T3SA^+$. At 12 days after inoculation, brains and hearts were resected, and whole-organ RNA was isolated and used as a template to generate cDNA. Levels of IFN-β and GAPDH cDNA were assessed by real-time PCR. The results are expressed as the mean ratio of IFN-β cDNA to that of GAPDH for 2 animals. Error bars indicate SDs.

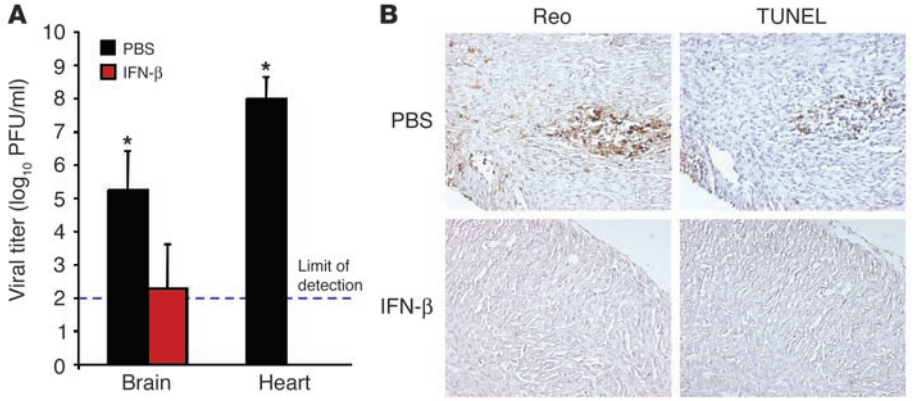

Figure 9
Reovirus replication and apoptosis in infected p50$^{-/-}$ mice following treatment with IFN-β. Newborn mice were inoculated intraperitoneally with either IFN-β or PBS 1 day prior to peroral inoculation with 10^4 PFU reovirus T3SA$^+$. Animals were treated with either IFN-β or PBS for an additional 9 days, and brains and hearts were resected. (**A**) Viral titers in the brain and heart. Organs were homogenized, and viral titers were determined by plaque assay. The results are expressed as the mean viral titers for 3 animals. Error bars indicate SDs. *P < 0.05 by Student's t test. (**B**) Histopathology of reovirus infection in the heart. Hearts of the reovirus-infected p50$^{-/-}$ animals represented in **A** were paraffin embedded, sectioned, and stained with polyclonal reovirus-specific antiserum or processed for TUNEL analysis. Original magnification, ×100. Brown staining indicates reovirus protein or fragmented DNA.

sample acquisition were used to prevent excessive heat loss. Electrocardiograms were digitally sampled and correspond to the usual surface lead I.

RNA isolation and real-time PCR. Two-day-old p50$^{+/+}$ and p50$^{-/-}$ mice were inoculated perorally with either 10^4 PFU T3SA$^+$ or PBS. Mice were euthanized, and brain and heart tissues were homogenized using a Dounce homogenizer. RNA was extracted from brain and heart homogenates using the TRIZOL RNA extraction protocol (Invitrogen Corp.). Three micrograms of RNA was used in a reverse-transcription reaction containing ×10 buffer, 25 mM $MgCl_2$, 100 μM dithiothreitol, and 1 U RNasin (Promega), 10 mM dNTPs, 50 μM random hexamers, and 1 U AMV reverse transcriptase (Promega). The reaction was incubated at 43°C for 1 hour and then at 95°C for 10 minutes.

Real-time PCR reactions were carried out using the Bio-Rad iCycler and iQ Supermix buffer containing DNA polymerase and SYBR Green (Bio-Rad Laboratories). Two to 3 replicate amplification reactions were performed in 96-well plates (Bio-Rad Laboratories). Each reaction contained 12.5 μl iQ Supermix buffer, 300 nM forward and reverse primers, and 1 μl cDNA in a final volume of 25 μl. Primers for the reactions were as follows: (a) IFN-β forward, 5′-GGAGATGACGGAGAAGATGC-3′, (b) IFN-β reverse, 5′-CCCAGTGCTGGAGAAATTGT-3′, (c) GAPDH forward, 5′-CAACTACATGGTCTACATGTTC-3′, and (d) GAPDH reverse, 5′-CTCGCTCCTGGAAGATG-3′. Cycling conditions were as follows: 95°C for 10 minutes and then 45 cycles at 95°C for 15 seconds, 60°C for 30 seconds, and 72°C for 15 seconds.

Data were analyzed using Bio-Rad iCycler PCR detection and analysis software version 3.0 (Bio-Rad Laboratories). DNA was quantitated using the standard curve method with the background subtracted. Known concentrations of cDNA were used to obtain the standard curve for each gene (concentrations between 0.0228 and 710 ng). A melting curve was determined for each sample to detect primer dimers, in which case data were not used. Results are expressed as values for IFN-β cDNA divided by those for GAPDH cDNA.

IFN-β treatment of mice. Two-day-old p50$^{-/-}$ mice were inoculated intraperitoneally with either 5×10^4 U IFN-β (Calbiochem) suspended in PBS containing 0.1% BSA or PBS alone in a volume of 25 μl 1 day prior to peroral inoculation with 10^4 PFU T3SA$^+$. Infected mice were treated daily for 9 days with either IFN-β or PBS. On day 10 following viral inoculation, animals were euthanized, and organs were removed. Organs were processed for determination of viral titer and histopathological analysis.

Animal husbandry and experimental procedures were performed in accordance with NIH Public Health Service policy and approved by the Vanderbilt University School of Medicine Institutional Animal Care and Use Committee.

Data analysis. Results are expressed as the mean ± SD. Differences between mean values were compared using unpaired Student's t tests as applied with Microsoft Excel software. P values less than 0.05 were considered statistically significant.

Acknowledgments

We thank Kelly Parman at the Vanderbilt Mouse Pathology Core Lab for tissue sectioning and Greg Hanley and Joan Richerson for expert veterinary care. We are grateful to Dean Ballard for review of the manuscript and Scott Baldwin and Luc Van Kaer for essential discussions. This research was supported by NIH Public Health Service awards T32 AI07474 (to S.M. O'Donnell and T. Valyi-Nagy), T32 HL07751 (to J.D. Chappell), T32 CA09385 (to J.C. Forrest), and R01 AI50080, and grants from the National Science Foundation (to E.S. Barton), the Vanderbilt University Medical Scholars Program (to M.J. Watson), the Vanderbilt University Research Council (to E.S. Barton and J.C. Forrest), and the Elizabeth B. Lamb Center for Pediatric Research. Additional support was provided by NIH Public Health Service awards CA68485 to the Vanderbilt-Ingram Cancer Center and DK20593 to the Vanderbilt Diabetes Research and Training Center.

Received for publication June 14, 2004, and accepted in revised form May 31, 2005.

Address correspondence to: Terence S. Dermody, Elizabeth B. Lamb Center for Pediatric Research, D7235 Medical Center North, Vanderbilt University School of Medicine, 1161 21st Avenue South, Nashville, Tennessee 37232, USA. Phone: (615) 343-9943; Fax: (615) 343-9723; E-mail: terry.dermody@vanderbilt.edu.

Jodi L. Connolly's present address is: Isis Pharmaceuticals, Carlsbad, California, USA.

Melissa J. Watson's present address is: Department of Surgery, UCLA Medical Center, Los Angeles, California, USA.

Erik S. Barton's present address is: Department of Pathology, Washington University School of Medicine, St. Louis, Missouri, USA.

J. Craig Forrest's present address is: Department of Microbiology and Immunology, Emory University School of Medicine, Atlanta, Georgia, USA.

Tibor Valyi-Nagy's present address is: Department of Pathology, University of Illinois-Chicago, Chicago, Illinois, USA.

1. Tyler, K.L., and Nathanson, N. 2001. Pathogenesis of viral infections. In *Fields virology*. D.M. Knipe and P.M. Howley, editors. Lippincott-Raven. Philadelphia, Pennsylvania, USA. 199–243.
2. Tyler, K.L. 2001. Mammalian reoviruses. In *Fields virology*. D.M. Knipe and P.M. Howley, editors. Lippincott-Raven. Philadelphia, Pennsylvania, USA. 1729–1945.
3. Virgin, H.W., Tyler, K.L., and Dermody, T.S. 1997. Reovirus. In *Viral pathogenesis*. N. Nathanson, editor. Lippincott-Raven. New York, New York, USA. 669–699.
4. Weiner, H.L., Powers, M.L., and Fields, B.N. 1980. Absolute linkage of virulence and central nervous system tropism of reoviruses to viral hemagglutinin. *J. Infect. Dis.* **141**:609–616.
5. Barton, E.S., et al. 2003. Utilization of sialic acid as a coreceptor is required for reovirus-induced biliary disease. *J. Clin. Invest.* **111**:1823–1833. doi:10.1172/JCI200316303.
6. Sherry, B., and Fields, B.N. 1989. The reovirus M1 gene, encoding a viral core protein, is associated with the myocarditic phenotype of a reovirus variant. *J. Virol.* **63**:4850–4856.
7. Sherry, B., and Blum, M.A. 1994. Multiple viral core proteins are determinants of reovirus-induced acute myocarditis. *J. Virol.* **68**:8461–8465.
8. Beg, A.A., et al. 1992. I kappa B interacts with the nuclear localization sequences of the subunits of NF-kappa B: a mechanism for cytoplasmic retention. *Genes Dev.* **6**:1899–1913.
9. Verma, I.M., Stevenson, J.K., Schwarz, E.M., Van Antwerp, D., and Miyamoto, S. 1995. Rel/NF-kappa B/I kappa B family: intimate tales of association and disassociation [review]. *Genes Dev.* **9**:2723–2735.
10. May, M.J., and Ghosh, S. 1997. Rel/NF-kappa B and I kappa B proteins: an overview [review]. *Semin. Cancer Biol.* **8**:63–73.
11. Beg, A., and Baltimore, D. 1996. An essential role for NF-κB in preventing TNF-α-induced cell death. *Science.* **274**:782–784.
12. Liu, T., Tang, Q., and Hendricks, R.L. 1996. Inflammatory infiltration of the trigeminal ganglion after herpes simplex virus type 1 corneal infection. *J. Virol.* **70**:264–271.
13. Van Antwerp, D., Martin, S., Kafri, T., Green, D., and Verma, I. 1996. Suppression of TNF-alpha-induced apoptosis by NF-kappaB. *Science.* **274**:787–789.
14. Abbadie, C., Kabrun, N., Bouali, F., Vandenbunder, B., and Enrietto, P. 1993. High levels of *c-rel* expression are associated with programmed cell death in the developing avian embryo and in bone marrow cells *in vitro*. *Cell.* **75**:899–912.
15. Jung, M., Zhang, Y., Lee, S., and Dritschilo, A. 1995. Correction of radiation sensitivity in ataxia telangiectasia cells by a truncated IκB-α. *Science.* **268**:1619–1621.
16. Lin, K.I., et al. 1995. Thiol agents and Bcl-2 identify an alphavirus-induced apoptotic pathway that requires activation of the transcription factor NF-kappa B. *J. Cell Biol.* **131**:1149–1161.
17. Dumont, A., et al. 1999. Hydrogen peroxide-induced apoptosis is CD95-independent, requires the release of mitochondria-derived reactive oxygen species and the activation of NF-kappaB. *Oncogene.* **18**:747–757.
18. Connolly, J.L., et al. 2000. Reovirus-induced apoptosis requires activation of transcription factor NF-κB. *J. Virol.* **74**:2981–2989.
19. Oberhaus, S.M., Smith, R.L., Clayton, G.H., Dermody, T.S., and Tyler, K.L. 1997. Reovirus infection and tissue injury in the mouse central nervous system are associated with apoptosis. *J. Virol.* **71**:2100–2106.
20. DeBiasi, R., Edelstein, C., Sherry, B., and Tyler, K. 2001. Calpain inhibition protects against virus-induced apoptotic myocardial injury. *J. Virol.* **75**:351–361.
21. Kretzschmar, M., Meisterernst, M., Scheidereit, C., Li, G., and Roeder, R.G. 1992. Transcriptional regulation of the HIV-1 promoter by NF-kappa B in vitro. *Genes Dev.* **6**:761–774.
22. Connolly, J.L., Barton, E.S., and Dermody, T.S. 2001. Reovirus binding to cell surface sialic acid potentiates virus-induced apoptosis. *J. Virol.* **75**:4029–4039.
23. Blatt, N.B., and Glick, G.D. 2001. Signaling pathways and effector mechanisms pre-programmed cell death. *Bioorg. Med. Chem.* **9**:1371–1384.
24. Sha, W.C., Liou, H.C., Tuomanen, E.I., and Baltimore, D. 1995. Targeted disruption of the p50 subunit of NF-kappa B leads to multifocal defects in immune responses. *Cell.* **80**:321–330.
25. Kontgen, F., et al. 1995. Mice lacking the c-*rel* proto-oncogene exhibit defects in lymphocyte proliferation, humoral immunity, and interleukin-2 expression. *Genes Dev.* **9**:1965–1967.
26. Weih, F., et al. 1995. Multiorgan inflammation and hematopoietic abnormalities in mice with a targeted disruption of RelB, a member of the Nf-κB/Rel family. *Cell.* **80**:331–340.
27. Sherry, B., Schoen, F.J., Wenske, E., and Fields, B.N. 1989. Derivation and characterization of an efficiently myocarditic reovirus variant. *J. Virol.* **63**:4840–4849.
28. Sherry, B., Baty, C.J., and Blum, M.A. 1996. Reovirus-induced acute myocarditis in mice correlates with viral RNA synthesis rather than generation of infectious virus in cardiac myocytes. *J. Virol.* **70**:6709–6715.
29. Sherry, B., Torres, J., and Blum, M.A. 1998. Reovirus induction of and sensitivity to beta interferon in cardiac myocyte cultures correlate with induction of myocarditis and are determined by viral core proteins. *J. Virol.* **72**:1314–1323.
30. Chu, W.M., et al. 1999. JNK2 and IKKbeta are required for activating the innate response to viral infection. *Immunity.* **11**:721–731.
31. Zamanian-Daryoush, M., Mogensen, T.H., DiDonato, J.A., and Williams, B.R. 2000. NF-kappaB activation by double-stranded-RNA-activated protein kinase (PKR) is mediated through NF-kappaB-inducing kinase and IkappaB kinase. *Mol. Cell. Biol.* **20**:1278–1290.
32. Fitzgerald, K.A., et al. 2003. IKKepsilon and TBK1 are essential components of the IRF3 signaling pathway. *Nat. Immunol.* **4**:491–496.
33. Sherry, B., Li, X.Y., Tyler, K.L., Cullen, J.M., and Virgin, H.W. 1993. Lymphocytes protect against and are not required for reovirus-induced myocarditis. *J. Virol.* **67**:6119–6124.
34. Maisch, B., Ristic, A.D., Hufnagel, G., and Pankuweit, S. 2002. Pathophysiology of viral myocarditis: the role of humoral immune response [review]. *Cardiovasc. Pathol.* **11**:112–122.
35. Gilmore, T.D. 1999. The Rel/NF-κB signal transduction pathway: introduction [review]. *Oncogene.* **18**:6842–6844.
36. Pahl, H.L. 1999. Activators and target genes of Rel/NF-kappaB transcription factors. *Oncogene.* **18**:6853–6866.
37. Govind, S. 1999. Control of development and immunity by Rel transcription factors in Drosophila [review]. *Oncogene.* **18**:6875–6887.
38. Furlong, D.B., Nibert, M.L., and Fields, B.N. 1988. Sigma 1 protein of mammalian reoviruses extends from the surfaces of viral particles. *J. Virol.* **62**:246–256.
39. Blackwell, T.S., et al. 2000. Multiorgan nuclear factor kappa B activation in a transgenic mouse model of systemic inflammation. *Am. J. Respir. Crit. Care Med.* **162**:1095–1101.
40. Tyler, K.L., Bronson, R.T., Byers, K.B., and Fields, B.N. 1985. Molecular basis of viral neurotropism: experimental reovirus infection. *Neurology.* **35**:88–92.
41. Rubin, D.H., and Fields, B.N. 1980. Molecular basis of reovirus virulence. Role of the M2 gene. *J. Exp. Med.* **152**:853–868.
42. Virgin, H.W., IV, Bassel-Duby, R., Fields, B.N., and Tyler, K.L. 1988. Antibody protects against lethal infection with the neurally spreading reovirus type 3 (Dearing). *J. Virol.* **62**:4594–4604.
43. Valyi-Nagy, T., Olson, S.J., Valyi-Nagy, K., Montine, T.J., and Dermody, T.S. 2000. Herpes simplex virus type 1 latency in the murine nervous system is associated with oxidative damage to neurons. *Virology.* **278**:309–321.
44. Rottman, J.N., et al. 2003. Temporal changes in ventricular function assessed echocardiographically in conscious and anesthetized mice. *J. Am. Soc. Echocardiogr.* **16**:1150–1157.